UNIVERSITY of
BRADFORD

Library

The University of Bradford Institutional Repository

http://bradscholars.brad.ac.uk

This work is made available online in accordance with publisher policies. Please refer to the repository record for this item and our Policy Document available from the repository home page for further information.

To see the final version of this work please visit the publisher's website. Access to the published online version may require a subscription.

An Indoor Path Loss Prediction Model using Wall Correction Factors for WLAN and 5G Indoor Networks

H.A. Obeidat[1], R. Asif[1], O.A. Obeidat[2], N.T. Ali[3], S.M.R. Jones[1], W.S. Shuaieb[1], M.A. Al-Sadoon[1], K.W. Hameed[1], A.A. Alabdullah[1], Y.A. Dama[4], and R.A. Abd-Alhameed[1]*

[1]School of Engineering and Informatics, University of Bradford, Bradford BD7 1DP, UK.
[2]College of Engineering, Wayne State University, Detroit, USA.
[3]Department of Electrical and Computer Engineering, Khalifa University, Abu Dhabi, UAE
[4]Department of Telecommunications Engineering, An Najah National University, Nablus, Palestine.

Corresponding author: Raed Abd-Alhameed (R.A.A.Abd@bradford.ac.uk)

Key Points:

- A modified Effective Wall Loss Model (EWLM) for indoor environment.
- Real time measurements and simulations for various indoor path loss models.
- Several frequency spectrum band were considered for evaluation purposes.

Abstract

A modified indoor path loss prediction model is presented, namely Effective Wall Loss Model (EWLM). The modified model is compared to other indoor path loss prediction models using simulation data and real-time measurements. Different operating frequencies and antenna polarizations are considered to verify the observations. In the simulation part, EWLM shows the best performance among other models as it outperforms two times the dual slope model which is the second-best performance. Similar observations were recorded from the experimental results. Linear attenuation and one slope models have similar behaviour, the two models parameters show dependency on operating frequency and antenna polarization.

1 Introduction

The ability to locate a target object in an indoor environment has many potential applications: e.g. in security, emergency services, health care and commercial fields (Pierleoni et al., 2016; Suits, Farmer, Ezekoye, Abbasi, & Wilson, 2014; R. Zhang, Hoflinger, & Reindl, 2013). However, it is difficult to provide accurate location by radio means because of the complex multipath propagation within buildings (Obeidat et al., 2016).

Multipath propagation of wireless signals within buildings has been extensively studied in the context of the deployment of cordless phones (Keenan & Motley, 1990) and wireless local area networks (WLAN) (Borrelli, Monti, Vari, & Mazzenga, 2004; Crow, Widjaja, Kim, & Sakai, 1997; Kong, Tsang, Bensaou, & Gao, 2004). Propagation from outdoors to indoors has been studied in the context of cellular networks (Damosso & Correia, 1999). More recently, there has been significant interest in developing indoor location technologies, in many cases relying on the opportunistic exploitation of available WLAN signals (Zekavat & Buehrer, 2011) and deploying WLAN in the mm-Wave band (Moraitis & Constantinou, 2004).

Propagation models have been developed and can be broadly categorised as either predicting median signal strength (path loss and shadowing) like Motley Keenan model (Keenan & Motley, 1990) or channel behaviour (fading across time or frequency) like Saleh Valenzuela model (Saleh & Valenzuela, 1987). Path loss models predict the signal level (averaged over several wavelengths or a wide bandwidth) at a given distance from the transmitter (Keenan & Motley, 1990), whilst channel models describe the stochastic or deterministic variation of the signal level (narrowband) and the time-dispersion (wideband) at that location (Saleh & Valenzuela, 1987). With the advent of multiple input, multiple output (MIMO) systems, spatial channel models have been introduced. The 3D indoor environment comprises walls and floors, windows and doors, corridors, stairwells and lift-shafts, as well as fixtures and furniture which can be regarded (using radar parlance) as clutter (Remcom, 2017a).

Radio propagation through this segmented and cluttered environment can usefully be visualised by a ray-optical model (Saunders & Aragón-Zavala, 2007). A complete physical spatial channel model describes the angles of departure and arrival of rays, the amplitude, delay, phase and polarisation between transmitting and receiving system. Rays include the direct path, which may or may not be obstructed, together with paths suffering combinations of specular and diffuse reflection, diffraction, scattering and transmission through walls, floors or other obstacles. Adjacent buildings can provide additional reflected paths.

The delay on each ray path is related to the path length, whilst the amplitude, phase and polarisation depend on the combination of spreading losses and losses due to transmission through, reflection from or diffraction around obstacles, which in turn depends on their structure and material electrical properties (Saunders & Aragón-Zavala, 2007). At frequencies above the UHF band, penetration and diffraction losses tend to increase (Wells, 1977). In the mmWave band surface roughness becomes more significant, leading to an increase in diffuse reflected components. However, the essential ray-optical geometry remains the same, so that multipath components have the same delay, even if they are more attenuated (Haneda et al., 2016; Pascual-García, Molina-García-Pardo, Martínez-Inglés, Rodríguez, & Saurín-Serrano, 2016).

This highly complex channel behaviour is captured by ray-tracing software. However, there are practical limits on the accuracy with which the detail of building structures or clutter can be characterised or the extent to which the material electrical properties can be accurately known (Obeidat et al., 2016). There are also compromises made in the number of ray paths that can be found by the software within the constraints of a reasonable run-time and memory requirement (REMCOM, 2017b).

The ray-optical view of the propagation mechanisms leads naturally to a description of the channel in terms of its impulse response as given by (Hashemi, 1993). In the indoor channel, rays have been observed to arrive in clusters, as modelled by (Saleh & Valenzuela, 1987). The clusters can be associated with angles of arrival and departure in developing spatial channel models (Spencer, Jeffs, Jensen, & Swindlehurst, 2000). The impulse response will vary with position and if the terminal (or clutter) is moving, this translates into time variation.

Despite the obvious underlying complexity of the indoor channel, (Keenan & Motley, 1990) looked to provide a straightforward engineering model for path loss. Their approach was to consider the various walls and floors obstructing the straight-line path between transmitter and receiver and to factor in a best-fit loss per wall or floor of each identifiable type, e.g. stud partition (drywall) or concrete block walls, suspended concrete floor beams or wooden floors, etc. When these losses were factored in, they found a residual free-space variation with

distance (i.e. power law index of two). A deficiency of their model was its tendency to over-predict loss where there are many floors or walls (presumably because there is an alternative, lower-loss path around those obstacles).

Other models have been proposed from simple power laws, two-slope or multi-slope models (Lott & Forkel, 2001) (Andrade & Hoefel, 2010) (Pahlavan & Levesque, 2005) to those that use the Keenan and Motley concept with some added sophistication to reduce the loss per floor as the number of floors increase (Serôdio et al., 2012). Waveguiding, e.g. along corridors can lead to path loss indices approaching one, whilst the presence of clutter within the first Fresnel zone of a ray can lead to indices of 4-6 beyond a break-point as for ground-wave propagation (Rappaort, 2002).

In this paper, several indoor path loss models and their associated parameters are examined and tested. A modified method named Effective Wall Loss Model (EWLM) to estimate the path loss is proposed. The performance of the proposed method was compared to other related methods in terms of various frequency spectrums covering WLAN and millimetre wave frequencies; the effect of antenna polarization was also studied. Simulated and measured test results were presented in which it shows the proposed method outperformed the other tested models. The organisation of this paper is as follow: Section 2 investigates different indoor path loss prediction models, Section 3 describes the experimental setup of the simulations and measurements and the procedure followed to estimate model parameters. Section 4 presents simulation and experimental results and a comparison between indoor path loss models and the modified model and finally conclusion is drawn.

2 Indoor Path Loss Models

Many models have been proposed in literature including one slope model (Lott & Forkel, 2001), dual slope model (Andrade & Hoefel, 2010), linear attenuation model (Davies, Simpson, & Mcgreehan, 1990), partitioned model (Alsindi, Alavi, & Pahlavan, 2009), Motley Keenan model (Keenan & Motley, 1990), averaged wall model (Lloret, López, Turró, & Flores, 2004), ITU-R P.1238 model (ITU, 2012) COST 231 indoor model (Pedersen, 1999) and dominant path model (Plets, Joseph, Vanhecke, Tanghe, & Martens, 2012).

2.1 One Slope Model (OSM)

A fast and simple model, also termed as simplified path loss model where the received power at a point is given by (Lott & Forkel, 2001):

$$P_r(dB) = P_0(dB) - 10n \log_{10}(d) \tag{1}$$

where P_0 is the received power at a 1 m away from the transmitter which can be estimated using free space formula or experimentally (Goldsmith, 2005), n is the path loss exponent which is calculated using interpolation (Zvanovec, Valek, & Pechac, 2003) and d is the distance from transmitter. Path loss is dependent on range (distance) and path loss exponent (Goldsmith, 2005). In (Alexander & Pugliese, 1983) various values of decay index n are presented, the values ranging from 1.2 due to waveguiding effects in corridors to 6.1 for dense office environment (Rappaort, 2002). In outdoor to indoor propagation at 1.7 GHz, decay index n found to be 1.495 for corridor single floor; 1.524 through corridors in that building and 3.25 for rooms single floor and 3.31 in rooms through building (Davies et al., 1990).

2.2 Linear Attenuation Model (LAM)

Authors in (Devasirvathan, 1991) proposed another approach, the experiments were carried out on range of frequencies (0.85, 1.9, 4 and 5.8 GHz), it was concluded that total loss L is the sum of free space loss L_{FS} and loss factor a in the range of (0.3 to 0.6 dB/m) depending on frequency and building (Devasirvathan, 1991).

$$P_r(dB) = P_0(dB) - 20 \log_{10}(d) - a \cdot d \tag{2}$$

where d represents distance in metre.

2.3 Dual Slope Model (DSM)

Propagation within indoor environment was categorized depending on first Fresnel zone clearance, the "*near transmitter propagation*" where no obstruction in the 1st Fresnel zone and the path loss exponent is less than 2 due to waveguiding, and "*breakpoint propagation*" when the furniture falls in the 1st Fresnel zone where path loss exponent becomes larger than 2, the model is shown in Equation 3 (Andrade & Hoefel, 2010).

$$P_r = P_0 - 10 \begin{cases} n_1 \log_{10}(d) & d < d_{bp} \\ n_1 \log_{10}(d_{bp}) + n_2 \log_{10}\left(\dfrac{d}{d_{bp}}\right) & d > d_{bp} \end{cases} \tag{3}$$

where n_1, n_2 are the path loss exponents and d_{bp} is the breakpoint distance. Calculation of the breakpoint distance is done either theoretically as in (Andrade & Hoefel, 2010) or experimentally as in (Nuangwongsa, Phaebua, Lertwiriyaprapa, Phongcharoenpanich, & Krairiksh, 2009).

2.4 Partitioned Model (PM)

In this model, path loss is estimated based on predetermined values of n and distance between transmitter and receiver (Pahlavan & Levesque, 2005):

$$P_r = P_0 - \begin{cases} 20 \log_{10} d, & 1m < d \leq 10m \\ 20 + 30 \log_{10} \dfrac{d}{10}, & 10m < d \leq 20m \\ 29 + 60 \log_{10} \dfrac{d}{20}, & 20m < d \leq 40m \\ 47 + 120 \log_{10} \dfrac{d}{40}, & d > 40m \end{cases} \tag{4}$$

2.5 ITU-R P.1238 Indoor Model

An empirical model accounts the losses due to penetration through floors within the same building (ITU, 2012):

$$L = 20 \log_{10} f_{MHz} + 10n \log_{10} \frac{d}{d_0} + L_f\big(N(F)\big) - 28 \tag{5}$$

Where $L_f\big(N(F)\big)$ is the floor penetration loss which varies with frequency, type of floor and number of floors between the transmitter and receiver $(N(F))$. Based on enormous

measurements, the model gives typical values for n and $L_f(N(F))$ for different indoor environments which are available in (ITU, 2012), in the case both the transmitter and receiver are in the same floor then $L_f = 0$.

2.6   Motley-Keenan Model (MKM)

The wide range of n makes the use of one slope model insufficient (Keenan & Motley, 1990), MKM considers the effect of walls and floors, including their types and numbers (Keenan & Motley, 1990) (Lima & Menezes, 2005).

$$L = L_{FS} + L_C + \sum_{i=1}^{I} N_{wi} L_{wi} + \sum_{j=1}^{J} N_{fj} L_{fj} \tag{6}$$

Where $L_{FS}, L_C, N_w, N_f, L_w, L_f, i$ and j are the free space loss, constant term (loss at $d_0 = 1\,m$), number of walls, number of floors, wall loss factor, floor loss factor, type of wall and type of floor respectively.

2.7   COST231 Indoor Model

A more sophisticated model is given by COST231, which adopts the concept of Keenan and Motley model (Pedersen, 1999). The model assumes a linear increase of loss as the number of walls increase, and non-linear increase of loss with respect to the number of floors as the average floor losses tend to decrease when the number of floors increase; the model is given in Equation 7 (Pedersen, 1999) (Serôdio et al., 2012):

$$L = L_{FS} + L_C + \sum_{i=1}^{I} N_{wi} L_{wi} + L_f n_f^{\left(\frac{(n_f+2)}{(n_f+1)}-b\right)} \tag{7}$$

Where L_C is the resultant wall losses obtained by applying multiple linear regression to the measurements, n_f is the number of encountered floors and b is an empirical constant, L_{wi} is wall losses of type i and L_f is the floor loss. An extension has been made so that individual wall losses decrease as the number of walls increases which gives better performance (Serôdio et al., 2012).

2.8 Dominant Path Model (DPM)

Dominant Path Model (DPM) is similar to Motley and Keenan method; however instead of considering the direct ray, the dominant rays are considered instead (Wölfle, Wol, & Landstorfer, 1997). It considers the main rays which contributes most of the energy, using this model will reduce the dependency of having a fine detailed simulated environment, it also reduce the computational time as it considers less rays (Wolfle & Landstorfer, 1998). Minimum losses for DPM computed as in Equation 8 (Plets et al., 2012):

$$L = L_{FS} + \sum_{i=1}^{k} WL_j + \sum_{j=1}^{p} w_I \tag{8}$$

Where L_{FS} is the free space loss, WL is cumulated wall losses, w_I is interaction loss which depends on type of wall, operating frequency, and the angle of bend made by the propagation.

2.9 Average Wall Model (AWM)

AWM was proposed by (Lloret et al., 2004) as a fast design model for indoor radio coverage where few measurements are required as they are collected one meter away from the transmitter and each wall in the facility. This model is similar to Motley Keenan model; however the way losses are calculated is different, losses from the same type of walls are averaged, the total loss after each wall is the result of multiplication of the average losses with total number of encountered walls. The first wall loss is estimated at 1 meter way from the wall by finding the difference between the path loss estimated from measurements and the losses due to free space propagation as shown in Equation 9 (Lloret et al., 2004):

$$W_1 = P_{r1} - P_0 + 20\log_{10}(d_1) \tag{9}$$

Where P_{r1} is the received signal strength (RSS) one meter from the first wall, and d_1 is the distance between the transmitter and the point which is located 1 m from the first wall. Losses of following walls are estimated similarly after excluding previous wall losses (Lloret et al., 2004). In order to exclude the multipath effect, the mean value for the losses of the same type of walls is given by:

$$W_{avg} = \frac{\sum_{i=1}^{v} W_i}{v} \tag{10}$$

where v is the total number of encountered walls. The path loss at distance d can be expressed as shown in Equation (11), where L is the number of encountered walls.

$$P_r(d) = P_0 - 20\log_{10}(d) - W_{avg} \cdot L \tag{11}$$

2.10 Effective Wall Loss Model (EWLM)

The Average Wall Model (AWM) captures the changes in the propagation environment; therefore, wall losses may be positive or negative. In fact, these losses can be considered as correction factors rather than losses. Using the "*average*" will superimpose the effect of all walls and then assume that all walls will contribute equally which is not necessary true. The main problem with this model is the assumption that the main source of signal fading are the walls; therefore, similar walls will affect the signal similarly. Although this is partially true especially for millimetre waves as will be shown later, there are many other sources that affect the signal strength (SS) level mainly multipath.

The AWM model superimposes the multipath effect; however, the effects of multipath fading give a fingerprint about how waves in specific region behaves. Also the concept of averaging does not reflect a scientific impact as it is unlikely that the last wall loss will affect the measurements at locations much before that wall. Another limitation to the AWM that it does not consider the effect of Line-of-Sight (LOS) propagation where path loss exponent will be less than the free space path loss exponent due to waveguiding effect.

Due to these limitations, we adopt the AWM with two modifications: first, the path loss estimated at a point depends on the losses due to the encountered wall only rather than using the concept of averaging. The second modification includes the effect of path loss exponent in the region between the transmitter and the first wall which may be affected by waveguiding effect. For Non-line-of-Sight propagation areas (NLOS) the effect of path loss exponents is

already embedded with the wall correction factors. In order to distinguish it from the AWM, we refer to the last modification as Effective Wall Loss Model (EWLM). The path loss at distance *d* can be expressed as:

$$P_r(d) = P_0 - 10n \log_{10}(d) - \sum_{i=1}^{L} W_i \qquad (12)$$

Where *n* is 2 for NLOS propagation, while for LOS propagation it is estimated by best fitting, *L* is the number of encountered walls. It is worth mentioning that W_{avg} in Equation 11 depends on total wall losses of the same type; therefore, applying Equation 11 will consider the effect of walls before and after the point of interest. Walls after the point of interest are unlikely to contribute significantly to the RSS compared to those before the point; therefore, EWLM considers the effect of walls which are only before the point of interest. Even if the walls are of the same type both models will work differently as shown in the incoming sections; however, they will have similar results after the last encountered wall where ($W_{avg} \cdot v = \sum_{i=1}^{v} W_i$).

3 Methodology and Experimental setup

In the first part of our analysis, different indoor path prediction models were examined and compared to the EWLM using data obtained from ray tracing software called Wireless Insite® which has been extensively validated, especially for the UHF band (Meðeđović, Veletić, & Blagojević, 2012) and for 802.11ac frequencies (Dama, Abd-Alhameed, Salazar-Quinonez, Jones, & Gardiner, 2011). The adopted environment for the experiment was the third floor in Chesham building in Bradford University. The model for the building was constructed using the software.

Transmitter and receivers implemented in the environment are both omnidirectional, transmitted power was set to 20 dBm, while receiver sensitivity was set to -120 dBm. Five frequencies were examined including (2.4 GHz, 5.3 GHz, 28 GHz, 60 GHz and 73.5 GHz), their corresponding bandwidths are (0.084 GHz (Wu, Hsiao, Lu, & Chang, 2004), 0.12 GHz (Koivunen et al., 2007), 0.8 GHz (Maccartney, Rappaport, Sun, & Deng, 2015), 2.15 GHz (Technologies, 2017) and 2 GHz (Instruments, 2016) respectively, those frequencies have wide usage for indoor applications. We also investigated two types of polarization: vertical polarisation (VP) and circular polarization (CP), settings for Wireless Insite are given in Table 1.

In the second part of the experiments, real time measurements have been collected from WLAN access points (AP) distributed in the 3rd floor of Chesham building at the University of Bradford, those APs support Wi-Fi coverage on both 2.4 GHz and 5.3 GHz bands. In these experiments, three APs were considered as shown in Figure 1. All APs are similar, this includes the transmitter power, types of antenna used and bandwidth. For each AP, data are collected over two routes, measurements are taken at 1 meter height with 0.5 m spacing between each two measurements. The heights for AP1 is 2.2 m while for AP2 and AP3 the heights are 2.75 m. A WLAN scanner software called *inSSIDer*® was used to collect the measurements using a laptop with a calibrated 802.11a/b/g/ac card adapter, these measurements are averaged to remove the effect of fast fading, the RSS reading is updated every one second.

This experiment was limited for a single floor only; in this case the comparison includes OSM, DSM, LAM, PM, MKM, AWM and EWLM (DPM is included in the experimental part only). For single floor analysis, the ITU model and the COST-231 model are the same as the OSM and MKM respectively, further analysis for multi floor propagation are subject for further publication.

A valid comparison between the different modelling approaches requires that each model is applied to the same dataset in order to predict parameters. MATLAB is used to estimate the parameter values which provide the best fit to the data. Typical data are shown in Table 2. Table 3 summarises the different parameters used in each model.

Having generated the best fit parameters, these same values are used to predict the RSS along various routes. Model predicted RSS is calculated for each model using the equations in Section 2. The model-predicted RSS values for each route and frequency are compared with the data available from measurements and from Wireless InSite ray-tracing simulations.

Error vector distance is estimated between the model-predicted RSS values and the data from Wireless Insite simulations or measurements, then the Root Mean Square Error (RMSE) of this vector is calculated. The smaller the RMSE the better model performance.

In (Plets et al., 2012) authors formulate a generalised formula for the DPM to be applied for different types of building. Since Ray tracing and DPM are two distinct approaches to estimate SS, analysis for DPM is performed only on data collected from real time measurements. In the experimental part DPM results were compared to other models at both investigated frequencies. As recommended by authors in (Plets et al., 2012), DPM parameter values are taken from (Plets et al., 2012) and (Y. Zhang & Hwang, 1994).

It's worth mentioning that for the EWLM after each wall the model makes a correction factor either by adding gain or adding loss in order to fit the simulations/measurements. MKM assumes values for wall losses such that it makes the best fit for all simulations (in case of ray tracing) or measurements (in case of actual measurements) from all different routes, these losses are different from correction factors used by AWM and EWLM. OSM, DSM and LAM look for the best fitting for the simulations/measurements (different values for n and a can be used to describe the propagation channels within corridors and rooms. DPM use the cumulated wall losses and interaction losses; this is required to identify all possible direct paths and their corresponding bent angles as mentioned in (Plets et al., 2012). After that, cumulated wall losses and interaction losses are calculated using Table 4 and Figure 6 in (Plets et al., 2012).

As shown in Figure 1, measurements are taken from AP1 on the yellow routes, while they were taken from AP2 and AP3 on the red and blue routes respectively. The simulation includes many routes within the floor to cover different scenario and to verify the observations. Figure 2 shows a 3D view for the simulated environment; the colours are different for different features. Material dependence on operating frequency plays a major role in determining the radio coverage, as shown in Equation 13, the attenuation rate A (dB/m) is a function of conductivity σ and relative permittivity ε_r (ITU, 2015).

$$A = \begin{cases} 1636 \dfrac{\sigma}{\sqrt{\varepsilon_r}} & Dielectric \\ 545.8\sqrt{\sigma f_{GHz}} & Conductor \end{cases} \tag{13}$$

However both ε_r, σ are functions of the operating frequency as shown in Equations 14 and 15 respectively (ITU, 2015):

$$\varepsilon_r = \alpha f_{GHz}^{\beta} \tag{14}$$

$$\sigma = \gamma f_{GHz}^{\delta} \tag{15}$$

Where α, β, γ and δ are given by (ITU, 2015). As the operating frequency is changing, the interaction between waves and building material will change accordingly. Table 4 shows the values of ε_r and σ adopted in our experiment which are calculated using Equations 14 and 15.

4   Results and Discussion

4.1   Simulation Results

Table 5 summarises the simulation results for the examples presented in this paper, where row 1, 2, 3 and 4 represent RMSE for the examined indoor path loss prediction models of different routes in the environment at 5.3 GHz using VP antenna, 2.4 GHz using VP antenna, 73.5 GHz using CP antenna and 60 GHz using CP antenna respectively.

A comparison between different indoor path loss models at 5.3 GHz using vertical polarized antenna is shown in Figure 3; RMSE of the examined models are presented in Table 5, row 1. In this scenario, the EWLM outperforms other models as it was able to capture the changes in the environments. After each wall, the model makes a correction factor either adding gain or adding loss to fit the simulation data. In the AWM, the first two walls loss give positive gain to the averaging, as a result the model underestimates SS fading. MKM works fine as long the signal level follows semi-monotonic decrease.

As provided from the RMSE values, both OSM and LAM models show low performance; this may be due the difficulty to model the simulation data with a monotonic function. The DSM uses two slopes to describe the changes in the environment. Due to this flexibility, it has better results compared to OSM. Finally, the PM has different path loss exponents; however, it shows good performance if the test environment has similar path loss exponents to the model.

In Figure 4, the mean SS level decays slowly with distance, the RMSE of the examined models are presented in Table 5, row 2. EWLM model has the best performance; while OSM has the second best performance as the path loss exponent found to be around 2, this may be regarded due to waveguiding effect. The DSM has lower performance compared to OSM, although this model uses two path loss exponents which gives more flexibility, the model requires more data in order to provide accurate prediction. In this scenario and using lower frequencies, there will not be much losses due to propagation through drywall. As a result, the correction factors will have less significant effect; however considering the waveguiding

effect gives EWLM advantage over AWM as seen in Figure 4. While at higher frequencies, propagation through these walls will lead to greater losses; therefore, the correction factors will have more impact as shown in Figure 5.

In Figure 5 simulation results are presented for the same route whose results are shown in Figure 4; but at higher frequency. The RMSE of the examined models are presented in Table 5, row 3. In comparison, models which use free space path loss exponent (n=2) and add walls losses (i.e. EWLM, AWM and MKM) or models use fixed values of n like PM are both expected to have better performance, this is due to fact that wall losses tend to be greater as frequency increases as indicated in the metrics Table 5. At higher frequencies, walls contribute to loss significantly; as a result, the OSM will have less accurate estimation while the DSM has advantage from having two slopes and hence shows more stability.

In Figure 6 many models predicts the SS sufficiently in the first 11 m and in the last 7 m; however SS level follows unpredicted behaviour in the 11-14 m window where most of them find difficulty to capture these changes as provided by their corresponding RMSE values which are presented in Table 5, row 4, in this scenario the MKM has the best performance.

Through the experiment, the average RMSE shows an increase as frequency increases as shown in Table 6. Almost all models have larger RMSE values at 28 and 60 GHz compared to the 73.5 GHz band. This increase varies from one model to another as shown in the table, in performance comparison for the models using VP antenna CP antenna, the table shows that for AWM, OSM, MKM, LAM and PM have higher RMSE for VP antenna. The EWLM has similar performance for both types of antenna especially for mm-wave frequencies.

As mentioned earlier, MKM adopts values for wall losses to give best fit for simulations; Table 7 shows the values given for drywalls and concrete walls for the used frequencies; losses for concrete walls and drywall tend to increase with frequency. They also tend to be larger in the case of VP compared to CP; this is because when a singly reflected CP signal with angle of incidence is greater than Brewster angle it will be orthogonal to the line of sight (LOS) component which leads to reduction in multipath interference (ITU, 2012), moving further away from the transmitter incidence angles become greater than the Brewster angle.

Figure 7 presents a RSS comparative behaviour with distance between VP and CP at 28 GHz, the higher SS in the CP case as receiver is moving further away from the AP can be explained by the effect of the multipath interference reduction as mentioned above. As shown in the incoming discussion, the examined model parameters are found to have less values in the case of CP.

The average path loss exponent versus operating frequency for OSM is plotted in Figure 8; for VP antenna, n tends to increase as frequency increases. However, in the case of CP antenna average value of n tends to decrease as frequency exceeds 28 GHz. This is may be explained due to radio coverage reduction occurred as frequency increased; hence, a lower value for n is obtained.

The value of n for the corridor shown in Figure 1 tends to have slight dependency on the examined frequencies as it has almost fixed value equivalent to 0.9 in the case of VP and (0.6-0.9) in the case of CP.

Path loss exponent is influenced by changes in frequency, polarization and depending on route location within the floor. For example, using 60 GHz and CP antenna, n in corridor routes due to waveguiding effect found to have a value of 1, while using VP antenna for the same route it has a value of 1.7. In the case where path is between rooms, where walls are made from concrete, using VP antenna, n reached a value of 5.

The relationship between average attenuation factor and frequency for LAM model is shown in Figure 9. As expected a increases as frequency increases, VP antenna has higher attenuation factor than circular polarization antenna. The mean value for a for VP and CP are: 0.67 dB/m and 0.367 dB/m respectively. Considering Figure 8 and Figure 9, a similarity between OSM and LAM is observed, as the variation of n and a are very similar for many routes on different frequencies and polarization.

This also is proved by Figure 10, as shown both models have similar performance provided from their corresponding RMSE for almost 40% of tested scenarios. Whilst OSM has better performance for frequencies 2.4, 5.3 and 28 GHz, LAM has better performance for frequencies over 28 GHz. The figure also presents PM performance which shows the poorest performance among all the models due to its limitation by having fixed path loss exponents over predefined distances; however the model seems to have better performance for 60 and 73.5 GHz.

A comparison between OSM, DSM and MKM is demonstrated in Figure 11. DSM outperforms both OSM and MKM as it has less RMSE compared to OSM for almost 72.5 % of tested scenarios and less RMSE compared to MKM for 60.8 % of tested scenarios. For low frequencies range of this experiment DSM outperforms MKM, while for millimetre waves MKM has better performance. This can be regarded to the effect of wall losses in SS fading which is considered by MKM. OSM and DSM show similar pattern with obvious advantage for the DSM, due to the latter flexibility as it has two values for n. The model can capture propagation changes in the environment more efficiently; the gap between the two models increases as frequency increases. On the other hand, MKM outperforms OSM as it has less RSME for almost 62.75 % of tested scenarios. It can also be observed that for higher frequencies, both DSM and MKM are preferable compared to OSM.

A comparison between EWLM, AWM and MKM is shown in Figure 12. EWLM shows better performance than MKM and AWM for almost 78.4% and 80.4% of tested scenarios respectively. The model has such advantage because the use of effective wall correction factors enhances SS prediction significantly. When comparing AWM with MKM, the former has less RMSE for almost 56.9% of tested scenarios. The AWM has also better performance in the 2.4, 5.3, 73.5 GHz regions, while it has comparable performance at the 60 GHz. It may be observed that at 28 GHz the AWM has lower performance. This is due to the effect of averaging with makes SS prediction less accurate at higher frequencies; however, as frequency increases the radio wave coverage becomes smaller. Therefore, the encountered walls become less, in such case the AWM works better. It was also observed that when all the

walls encountered are from the same type (i.e. either all are concrete or drywall) the performance of AWM is always lower than EWLM.

Considering models performance at all frequencies, DSM shows the second-best performance, a comparison between EWLM and DSM is presented in Figure 13; the metrics show better performance for EWLM as it has less RMSE for almost 66.67% of the tested scenarios. At 2.4 GHz DSM has comparable performance with the EWLM; however, as the operating frequency increases EWLM tends to have better results. This is due to considering effects of wall losses as mentioned earlier.

The average error for most models reaches maximum at 28 GHz. This can be explained as follow: as the frequency increases the radio coverage tends to become shorter, so it will have less error. Although at 28 GHz the coverage was less compared to 5.3 and 2.4 GHz; however, signal variations tend to be greater; therefore, errors are greater. While at 60 GHz and 73.5 GHz the radio coverage becomes much smaller; thus, errors are less compared to 28 GHz. One interesting observation noted, although both 60 GHz and 73.5 GHz share the same radio coverage, errors at 60 GHz are greater; this might be because the 60 GHz has more fluctuations compared to 73.5 GHz.

Although AWM has the advantage for being fast prediction model, it comes at the expense of accuracy. EWLM combines accuracy and speed. The PM has the lowest performance as it has pre-determined values for n, in comparison to EWLM it has less RMSE for less than 7.8% of tested scenarios.

The order of the best models according to their RMSE values is EWLM, DSM, MKM, AWM, OSM, LAM then PM; their respective average RMSE for all scenarios at all frequencies are shown in Table 8. EWLM has the best performance while PM has the worst performance.

Table 8 also shows the percentage of having the least RMSE for each model over all scenarios and frequencies; EWLM was considered as the one with the least RMSE for 51% of all scenarios while DSM has a percentage of 22%. Considering these results EWLM is an attractive model especially for millimetre wave frequency usage.

A comparison between the EWLM with no modification (where n=2 for all scenarios) and with enhancement (n is estimated by best fitting for LOS propagation and 2 for NLOS propagation) is presented in Figure 14, on average the RMSE for all frequencies had reduced by about 1 dB. Compared to other models "EWLM with no modification" had the least RMSE for 27.45% of all tested scenarios; however by considering the effect of LOS and waveguiding effect the percentage was enhanced to 51% as mentioned above.

In Figure 15 correction factor for concrete wall found to increase linearly with increasing the operating frequency in the range of (5.3-60 GHz) for both VP and CP cases. While correction factor for drywall tend to vary linearly with frequency range (2.4-73.5 GHz) for VP and in the range (5.3-60 GHz) for CP. For both types of wall, mean wall correction factor tends to be larger for VP compared to CP especially for large frequencies.

4.2 Experimental Results

The experimental study in this paper includes same models investigated in the simulation part in addition to DPM. Figure 1 represents measurements collected in 3rd floor, measurements were taken in different routes to examine more possible scenarios where walls are made from concrete and drywalls. It was observed that radio coverage for 5 GHz band is slightly larger than radio coverage for 2.4 GHz band, this can be explained as the former's effective radiated power (ERP) is much larger.

A comparison between investigated models is presented in Figure 16 where data are collected from route 2-2 (shown in Figure 1) at 5.3 GHz. It's expected to have a semi-monotonic RSS decaying. The RMSE for the EWLM, AWM, OSM, LAM, PM, MKM DSM and DPM in dB are: 4.2892, 5.52, 6.067, 5.4572, 7.62, 5.978, 4.9378 and 14.1928 respectively.

As the first wall is close to the transmitter the correction factor will add more accurate estimation to the results, EWLM has the best performance, the AWM also shows a good resolution; however it shows less performance compared to EWLM, this is due to the effect of last wall loss on averaging which cause the SS prediction to be pessimistic. Since the RSS follows a semi-monotonic decaying OSM, LAM, MKM and DSM show a good performance, the PM use fixed values for n, which underestimate the actual losses in this scenario. DPM uses predefined values for building wall losses; however the performance was pessimistic, this may be due to the wall losses recommended are not for universal use as authors claims; also the model has no difference in performance from other wall loss models if the direct path between the transmitter and the receiver is the path with least losses.

A comparison between all presented models is introduced in Figure 17, the total error for all routes are averaged. For the 2.4 GHz, as shown from the figure and Table 9, the OSM, DSM and EWLM have the best performance. Similar to observed results from simulation part, EWLM has the most stable performance as the maximum error did not exceed 6.1102 dB and the standard deviation (STD) of errors is around 1.156 dB. PM, DPM and MKM have low accuracy, as the maximum error exceeds 15 dB, 14 dB and 11 dB respectively, while their STD are 3.4306 dB, 4.1256 dB and 2.9566 dB respectively. The LAM and AWM have comparable performance as provided by their metrics.

Similar to PM, DPM uses predefined wall losses; therefore, the performance was poor as seen by the presented metrics. The advantage of using this model is limited to the scenarios where the transmitter and receiver are separated by one/multi walls and there is another path which encounters less number of walls; however, in many cases the best path is the shortest in distance between the transmitter and receiver which return this model to be similar to multi-wall models.

Using higher operating frequency, the EWLM has the best performance provided that it has the lowest values for all metrics as shown in Table 10; the metrics are consistent with the observed results in the simulation part. The AWM has the second-best performance and still show good results in terms of accuracy and stability. The DSM and LAM show comparable performances. The former performance degraded with increasing frequency; however, it still have stable and accurate estimation.

The OSM suffers from poor accuracy this is because of wall losses at higher frequency which requires more than one path loss exponent to have accurate estimation. The MKM still suffer from instability; however, it has better performance at 5.3 GHz this is due to the more effect contribution from the walls at higher frequencies which have larger values as frequency increases as shown in Table 11. DPM has similar behaviour to what was observed at 2.4 GHz; typical values used for wall losses using DPM are presented in Table 11.

Path loss exponent increases as operating frequency increases. Among all tested routes, measurements provided an evidence of path loss exponent dependency on the operating frequency. As observed from the measurements, n varies in the range of (1.93-3.3) at 2.4 GHz and in the range of (3.37-4.35) at 5.3 GHz. The averaged path loss exponent found to be 2.83, 3.89 at 2.4 GHz and 5.3 GHz respectively. Linear attenuation factor also shows an increase as the operating frequency increases. Among the six tested routes, measurements from five routes provided an evidence of linear dependency of the attenuation on the operating frequency; a varies in the range of (0.4-1.6) at 2.4 GHz and (1.2-2.5) at 5.3 GHz. The average attenuation factor for the 2.4 GHz and 5.3 GHz are 0.8166 and 1.6 respectively.

The averaged RMSE for all scenarios and frequencies are given in Table 12; among all scenarios, EWLM has the lowest RMSE for almost 50% of tested scenarios, whilst DSM has the lowest RMSE for 16.667% of tested scenarios. EWLM tends to have better performance as the frequency increase that seems to be consistent with the simulation results. Similar to observations in Figure 15, wall correction factor for concrete tends to increase more rapidly as frequency increased while for drywall the steep was smoother.

5 Conclusions

A modified indoor path loss prediction model has been presented using ray tracing software and then verified experimentally for 2.4 and 5.3 GHz WLAN frequency bands. In the simulation part, the model was examined and compared to other indoor path loss models at 2.4, 5.3, 28, 60 and 73.5 GHz with different antenna polarization. In the experimental part, the model was compared to same models at 2.4 and 5.3 GHz. In the simulation part EWLM shows the best performance among other models for almost two times the second best model. Similar observations were recorded from the experimental results. DSM showed the second-best performance provided it is equipped with sufficient data points. OSM and LAM have similar behaviour, and the two models showed dependency on operating frequency and antenna polarization. The PM showed the poorest performance as it has fixed path loss exponents.

References

Alexander, S., & Pugliese, G. (1983). Cordless communication within buildings: Results of measurements at 900 MHz and 60 GHz. *British Telecom Technology Journal, 1*(1), 99-105.
Alsindi, N. A., Alavi, B., & Pahlavan, K. (2009). Measurement and Modeling of Ultrawideband TOA-Based Ranging in Indoor Multipath Environments. *IEEE Transactions on Vehicular Technology, 58*(3), 1046-1058. doi: 10.1109/TVT.2008.926071

Andrade, C. B., & Hoefel, R. P. F. (2010, 2-5 May 2010). *IEEE 802.11 WLANs: A comparison on indoor coverage models.* Paper presented at the Electrical and Computer Engineering (CCECE), 2010 23rd Canadian Conference on, Calgary, AB, Canada.

Borrelli, A., Monti, C., Vari, M., & Mazzenga, F. (2004). *Channel models for IEEE 802.11 b indoor system design.* Paper presented at the Communications, 2004 IEEE International Conference on.

Crow, B. P., Widjaja, I., Kim, L., & Sakai, P. T. (1997). IEEE 802.11 wireless local area networks. *IEEE Communications Magazine, 35*(9), 116-126.

Dama, Y., Abd-Alhameed, R., Salazar-Quinonez, F., Jones, S. M., & Gardiner, J. (2011). *Indoor Channel Measurement and Prediction for 802.11 n System.* Paper presented at the Vehicular Technology Conference (VTC Fall), 2011 IEEE.

Damosso, E., & Correia, L. (1999). Digital Mobile Radio Towards Future Generation Systems Communications. COST 231 Final Report. *CEC, Brussels, Belgium.*

Davies, R., Simpson, A., & Mcgreehan, J. (1990). Propagation measurements at 1.7 GHz for microcellular urban communications. *Electronics Letters, 26*(14), 1053-1055.

Devasirvathan, D. (1991, 23-25 Sept. 1991). *Multi-frequency propagation measurements and models in a large metropolitan commercial building for personal communications.* Paper presented at the Personal, Indoor and Mobile Radio Communications., IEEE International Symposium on, UK.

Goldsmith, A. (2005). *Wireless communications*: Cambridge university press.

Haneda, K., Tian, L., Asplund, H., Li, J., Wang, Y., Steer, D., . . . Kim, Y. (2016, 23-27 May 2016). *Indoor 5G 3GPP-like channel models for office and shopping mall environments.* Paper presented at the Communications Workshops (ICC), 2016 IEEE International Conference on, Kuala Lumpur, Malaysia.

Hashemi, H. (1993). The indoor radio propagation channel. *Proceedings of the IEEE, 81*(7), 943-968. doi: 10.1109/5.231342

Instruments, N. (2016). mmWave: The Battle of the Bands.   Retrieved 25/10/2016, from http://www.ni.com/white-paper/53096/en/

ITU, I. T. U. (2012). Propagation data and prediction methods for the planning of indoor radiocommunication systems and radio local area networks in the frequency range 900 MHz to 100 GHz *Recommendation ITU-R P.1238-7*. Geneva: ITU.

ITU, I. T. U. (2015). Effects of building materials and structures on radiowave propagation above about 100 MHz *Recommendation ITU-R P.2040-1*. Geneva: Electronic Publication.

Keenan, J., & Motley, A. (1990). Radio coverage in buildings. *British Telecom Technology Journal, 8*(1), 19-24.

Koivunen, J., Almers, P., Kolmonen, V.-M., Salmi, J., Richter, A., Tufvesson, F., . . . Vainikainen, P. (2007). Dynamic multi-link indoor MIMO measurements at 5.3 GHz.

Kong, Z.-n., Tsang, D. H., Bensaou, B., & Gao, D. (2004). Performance analysis of IEEE 802.11 e contention-based channel access. *IEEE Journal on Selected Areas in Communications, 22*(10), 2095-2106.

Lima, A. G., & Menezes, L. F. (2005, 25-25 July 2005). *Motley-Keenan model adjusted to the thickness of the wall.* Paper presented at the SBMO/IEEE MTT-S International Conference on Microwave and Optoelectronics, 2005., Brasilia, Brazil.

Lloret, J., López, J. J., Turró, C., & Flores, S. (2004, 20-22 Sept. 2004). *A fast design model for indoor radio coverage in the 2.4 GHz wireless LAN.* Paper presented at the Wireless Communication Systems, 2004, 1st International Symposium on, Mauritius, Mauritius.

Lott, M., & Forkel, I. (2001, 6-9 May 2001). *A multi-wall-and-floor model for indoor radio propagation.* Paper presented at the Vehicular Technology Conference, 2001. VTC 2001 Spring. IEEE VTS 53rd, Rhodes, Greece, Greece.

Maccartney, G. R., Rappaport, T. S., Sun, S., & Deng, S. (2015). Indoor Office Wideband Millimeter-Wave Propagation Measurements and Channel Models at 28 and 73 GHz for Ultra-Dense 5G Wireless Networks. *IEEE Access, 3*, 2388-2424. doi: 10.1109/ACCESS.2015.2486778

Međedović, P., Veletić, M., & Blagojević, Ž. (2012, 21-25 May 2012). *Wireless insite software verification via analysis and comparison of simulation and measurement results.* Paper presented at the MIPRO, 2012 Proceedings of the 35th International Convention, Opatija, Croatia.

Moraitis, N., & Constantinou, P. (2004). Indoor channel measurements and characterization at 60 GHz for wireless local area network applications. *IEEE Transactions on Antennas and Propagation, 52*(12), 3180-3189.

Nuangwongsa, K., Phaebua, K., Lertwiriyaprapa, T., Phongcharoenpanich, C., & Krairiksh, M. (2009, 6-9 May 2009). *Path loss modeling in durian orchard for wireless network at 5.8 GHz.* Paper presented at the Electrical Engineering/Electronics, Computer, Telecommunications and Information Technology, 2009. ECTI-CON 2009. 6th International Conference on, Pattaya, Chonburi, Thailand.

Obeidat, H. A., Dama, Y. A., Abd-Alhameed, R. A., Hu, Y.-F., Qahwaji, R. S., Noras, J. M., & Jones, S. M. (2016). A Comparison between Vector Algorithm and CRSS Algorithms for Indoor Localization using Received Signal Strength. *The Applied Computational Electromagnetics Society (ACES), 31*, 868-876.

Pahlavan, K., & Levesque, A. H. (2005). *Wireless information networks* (Vol. 93): John Wiley & Sons.

Pascual-García, J., Molina-García-Pardo, J.-M., Martínez-Inglés, M.-T., Rodríguez, J.-V., & Saurín-Serrano, N. (2016). On the importance of diffuse scattering model parameterization in indoor wireless channels at mm-wave frequencies. *IEEE Access, 4*, 688-701.

Pedersen, G. F. (1999). *COST 231-Digital mobile radio towards future generation systems*: European Commission.

Pierleoni, P., Pernini, L., Belli, A., Palma, L., Maurizi, L., & Valenti, S. (2016, 4-8 Sept. 2016). *Indoor localization system for AAL over IPv6 WSN.* Paper presented at the 2016 IEEE 27th Annual International Symposium on Personal, Indoor, and Mobile Radio Communications (PIMRC), Valencia, Spain.

Plets, D., Joseph, W., Vanhecke, K., Tanghe, E., & Martens, L. (2012). Coverage prediction and optimization algorithms for indoor environments. *EURASIP Journal on Wireless Communications and Networking, 2012*(1), 123.

Rappaort, T. S. (2002). *Wireless communications: principles and practice* (2 edition ed.). Upper Saddle River, NJ, USA: Prentice Hall.

Remcom. (2017a, 05 Jan 2017). Wireless Insite. from http://www.remcom.com/wireless-insite

REMCOM. (2017b). Wireless InSite Reference Manual (3.1.0 ed.). State College, Pennsylvania: REMCOM.

Saleh, A. A., & Valenzuela, R. A. (1987). A statistical model for indoor multipath propagation. *Selected Areas in Communications, IEEE Journal on, 5*(2), 128-137.

Saunders, S., & Aragón-Zavala, A. (2007). *Antennas and Propagation for Wireless Communication Systems: 2nd Edition*: John Wiley & Sons.

Serôdio, C., Coutinho, L., Reigoto, L., Matias, J., Correia, A., & Mestre, P. (2012, July 4 - 6, 2012). *A lightweight indoor localization model based on motley-keenan and cost.* Paper presented at the Proceedings of The World Congress on Engineering 2012, WCE 2012, London, U.K.

Spencer, Q. H., Jeffs, B. D., Jensen, M. A., & Swindlehurst, A. L. (2000). Modeling the statistical time and angle of arrival characteristics of an indoor multipath channel. *IEEE Journal on Selected Areas in Communications, 18*(3), 347-360. doi: 10.1109/49.840194

Suits, J. I., Farmer, C. M., Ezekoye, O. A., Abbasi, M. Z., & Wilson, P. S. (2014). Personal alert safety system localization field tests with firefighters. *The Journal of the Acoustical Society of America, 136*(4), 2166-2166.

Technologies, A. (2017). Wireless LAN at 60 GHz - IEEE 80211ad-Explained-Agilent-White-Paper.

Wells, P. I. (1977). The attenuation of UHF radio signals by houses. *Vehicular Technology, IEEE Transactions on, 26*(4), 358-362.

Wolfle, G., & Landstorfer, F. (1998). *Dominant paths for the field strength prediction.* Paper presented at the Vehicular Technology Conference, 1998. VTC 98. 48th IEEE.

Wölfle, G., Wol, G., & Landstorfer, F. (1997). Field Strength Prediction With Dominant Paths And Neural Networks For Indoor Mobile Communication.

Wu, J.-W., Hsiao, H.-M., Lu, J.-H., & Chang, S.-H. (2004). Dual broadband design of rectangular slot antenna for 2.4 and 5 GHz wireless communication. *Electronics Letters, 40*(23), 1461-1463.

Zekavat, R., & Buehrer, R. M. (2011). *Handbook of position location: Theory, practice and advances* (Vol. 27): John Wiley & Sons.

Zhang, R., Hoflinger, F., & Reindl, L. (2013). Inertial sensor based indoor localization and monitoring system for emergency responders. *IEEE Sensors Journal, 13*(2), 838-848.

Zhang, Y., & Hwang, Y. (1994). *Measurements of the characteristics of indoor penetration loss.* Paper presented at the Vehicular Technology Conference, 1994 IEEE 44th.

Zvanovec, S., Valek, M., & Pechac, P. (2003, 31 March-3 April 2003). *Results of indoor propagation measurement campaign for WLAN systems operating in 2.4 GHz ISM band.* Paper presented at the Antennas and Propagation, 2003.(ICAP 2003). Twelfth International Conference on (Conf. Publ. No. 491), Exeter, UK,.

Table 1 *Wireless Insite settings for the investigated scenario.*

Property	Setting
Number of reflections	6
Number of transmissions	4
Number of diffractions	1
Number of reflections before first diffraction	3
Number of reflections after last diffraction	3
Number of reflections between diffractions	1
Number of transmissions before first diffraction	2
Number of transmissions after last diffraction	2
Number of transmissions between diffractions	1
Ray tracing method	SBR
Propagation model	Full 3D

Table 2 *Example of data used to predict model parameters*

	Distance (m)	RSS (dBm)
1	1	-32.22
2	8	-34.89
3	11	-40.22
4	16	-44.23
5	27	-54.22
6	30	-57.25
7	41	-66.78
8	44	-71.4

Table 3 *Estimated model parameters*

Model	Estimated Parameters
One slope model	Path loss exponent n
Dual slope model	Path loss exponents (n_1, n_2)
Linear Attenuation Model	Attenuation factor (a)
Motley-Keenan model	Wall losses (L_w)
Dominant Path model	Interaction losses
Average wall model	Average wall losses $(W_{avg.})$
Effective wall loss models	Wall correction factors (W_i)

Table 4 *Material properties with frequency*

Frequency (GHz)	Concrete		Glass		Wood		Drywall	
	ε_r	σ	ε_r	σ	ε_r	σ	ε_r	σ
2.4	5.31	0.0662	6.27	0.0122	1.99	0.0120	2.94	0.0216
5.3	5.31	0.1258	6.27	0.0314	1.99	0.0281	2.94	0.0378
28	5.31	0.4838	6.27	0.2287	1.99	0.1672	2.94	0.1226
60	5.31	0.8967	6.27	0.5674	1.99	0.3784	2.94	0.2102
73.5	5.31	1.0568	6.27	0.7228	1.99	0.4703	2.94	0.2427

Table 5 *RMSE (in dB) of the examined error (Simulation part)*

	EWLM	AWM	OSM	LAM	PM	MKM	DSM
1	7.5665	10.4207	12.4458	10.8654	9.849	8.3017	7.8459
2	5.2859	6.4431	5.6997	6.4315	8.5297	6.1118	8.1126
3	5.2702	6.3659	9.1779	8.118	7.2313	5.549	6.5214
4	14.9072	15.6219	13.115	12.9068	12.5806	11.2973	14.746

Table 6 *Average RMSE (in dB) with frequencies for examined models*

Model	2.4 GHz		5.3 GHz		28 GHz		60 GHz		73.5 GHz	
	VP	CP	VP	CP	VP	CP	VP	CP	VP	CP
EWLM	**5.0722**	**5.6069**	**4.6899**	**6.25176**	**10.844**	**10.845**	**10.458**	**9.6559**	**8.6377**	**8.6780**
AWM	8.4641	7.1195	8.4319	10.2344	15.856	15.585	11.860	10.555	9.5655	8.8229
OSM	7.6314	7.811	9.0169	10.0235	15.451	13.589	13.741	11.72	13.811	11.089
LAM	8.2767	8.4406	9.5144	10.5070	16.672	14.114	12.976	11.815	13.596	11.141
PM	16.527	15.743	16.886	15.4893	16.91	16.165	14.288	12.386	15.266	12.471
MKM	9.8295	8.6542	10.093	11.0623	13.383	12.35	11.260	10.002	9.6996	9.0939
DSM	5.752	6.1476	7.4956	8.6941	12.593	13.785	11.342	10.078	11.137	9.3423

Table 7 *Wall losses using MKM*

Frequency (GHz)	VP		CP	
	Drywall	**Concrete**	**Drywall**	**Concrete**
2.4	1	4	1	3
5.3	1	6	1	5
28	3	7	1	8
60	1	21	1	10
73.5	3	20	1	13

Table 8 *Percentage of having the least RMSE (ordered by average RMSE)*

Model	Percentage of the least RMSE	Average RMSE
EWLM	51%	7.6793
DSM	22%	9.26586
AWM	9.5%	10.4518
MKM	9.5%	10.5112
OSM	6%	10.9781
LAM	0%	11.3626
PM	2%	15.4435

Table 9 *Statistical metrics (in dB) between measured and simulated data for the presented models at 2.4 GHz*

Model	Max. Error	Min. Error	STD	RMSE
EWLM	6.1102	2.9334	1.1560	4.3707
AWM	8.4596	3.0472	2.0748	5.7672
OSM	6.5999	3.4202	1.2227	4.1568
LAM	8.1856	3.8566	1.7045	5.54635
PM	15.4375	5.7927	3.4306	10.159
MKM	11.4639	3.7119	2.9566	7.4469
DSM	7.0396	3.123	1.4079	4.6875
DPM	14.3069	4.3167	4.1256	7.7433

Table 10 *Statistical metrics between measured and simulated data for the presented models at 5.3 GHz*

Model	Max. error	Min. error	STD	RMSE
EWLM	4.6941	2.4044	0.7903	3.60744
AWM	5.6672	2.5276	1.2646	3.9943
OSM	8.4177	4.4267	1.3921	5.7298
LAM	6.2044	3.3204	1.121	5.0591
PM	14.1389	7.62	2.2813	10.9763
MKM	9.0968	3.0752	2.1387	5.0392
DSM	6.6239	4.0949	0.973	4.7900
DPM	14.1928	3.9692	3.7557	7.7599

Table 11 *Wall loss using MKM and DPM**

Frequency	MKM		DPM	
	Drywall	Concrete	Drywall	Concrete
2.4 GHz	4	4	2	10
5.3 GHz	3	12	7.5	12.5

*Wall losses using DPM from (Y. Zhang & Hwang, 1994) (Plets et al., 2012).

Table 12 *Averaged RMSE (in dB) for all models*

Model	Average RMSE
EWLM	3.9890
AWM	4.8808
OSM	4.9433
LAM	5.3027
PM	10.5681
MKM	6.2431
DSM	4.7388
DPM	6.7379
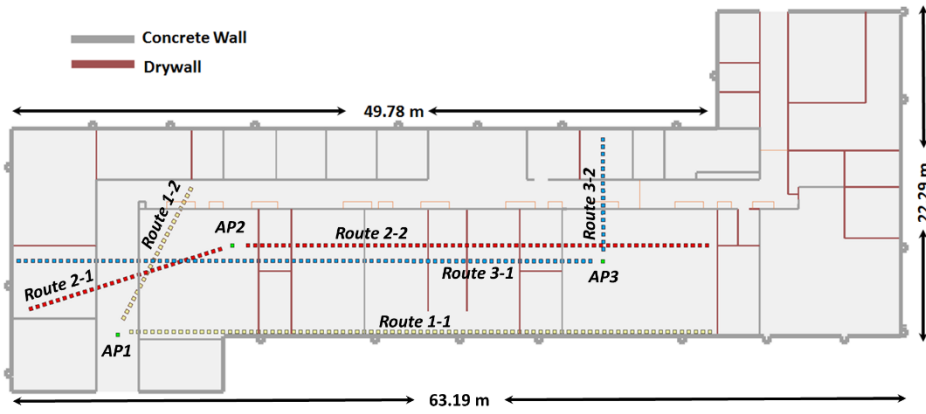
Figure 1: Experimental routes in 3rd floor Chesham building at the University of Bradford.
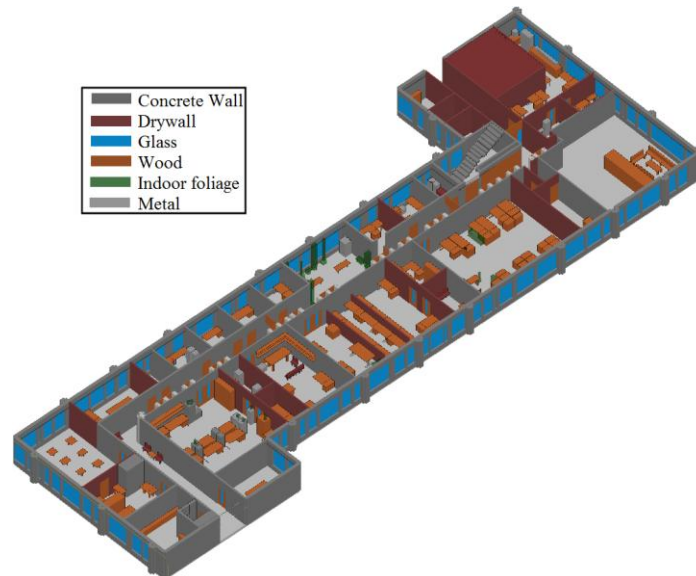
Figure 2: Simulated environment for 3rd floor in Chesham building, University of Bradford.
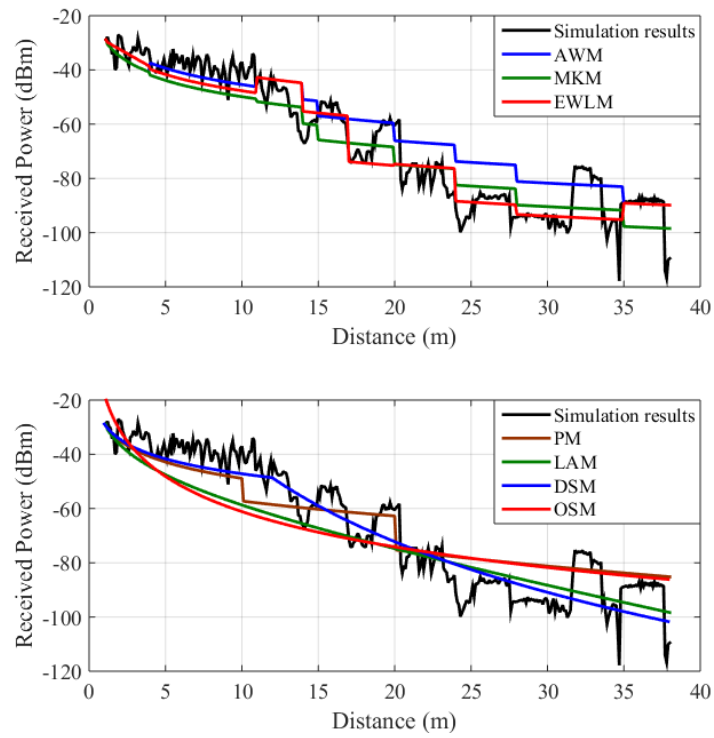
Figure 3: Indoor path loss prediction models comparisons for a route in the environment at 5.3 GHz using vertical polarized antenna.
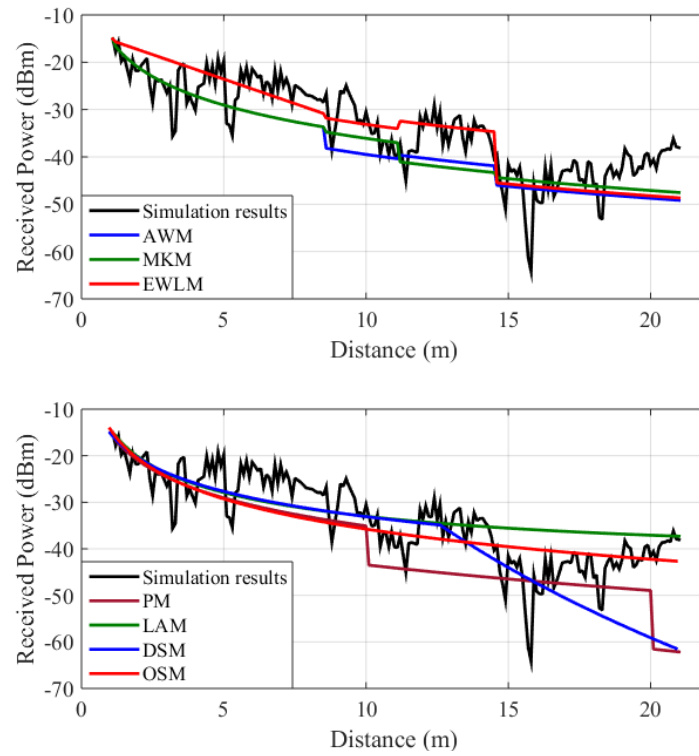
Figure 4: Indoor path loss prediction models comparisons for a route in the environment at 2.4 GHz using vertical polarized antenna.
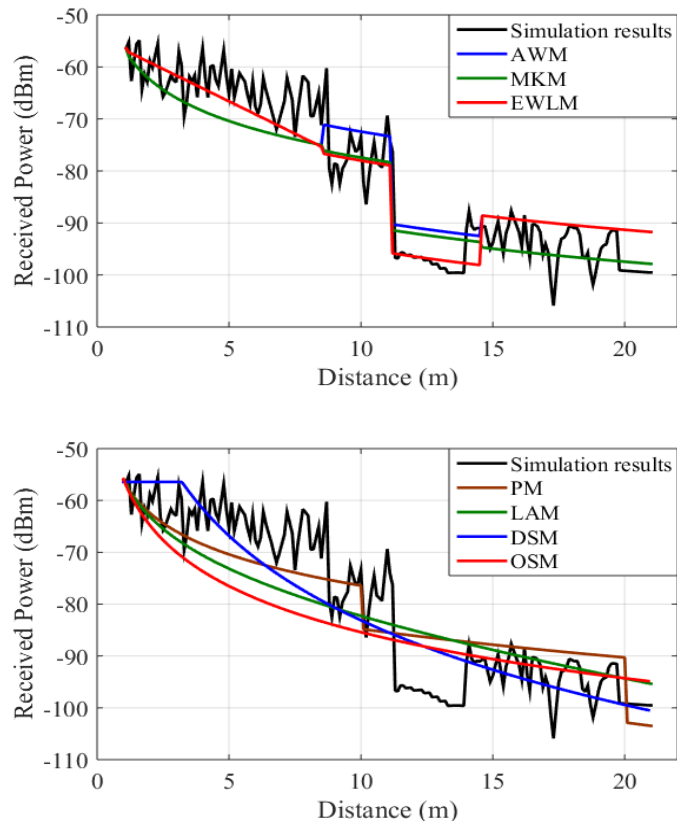
Figure 5: Indoor path loss prediction models comparisons at 73.5 GHz and circular polarization for the same route in Figure 4.
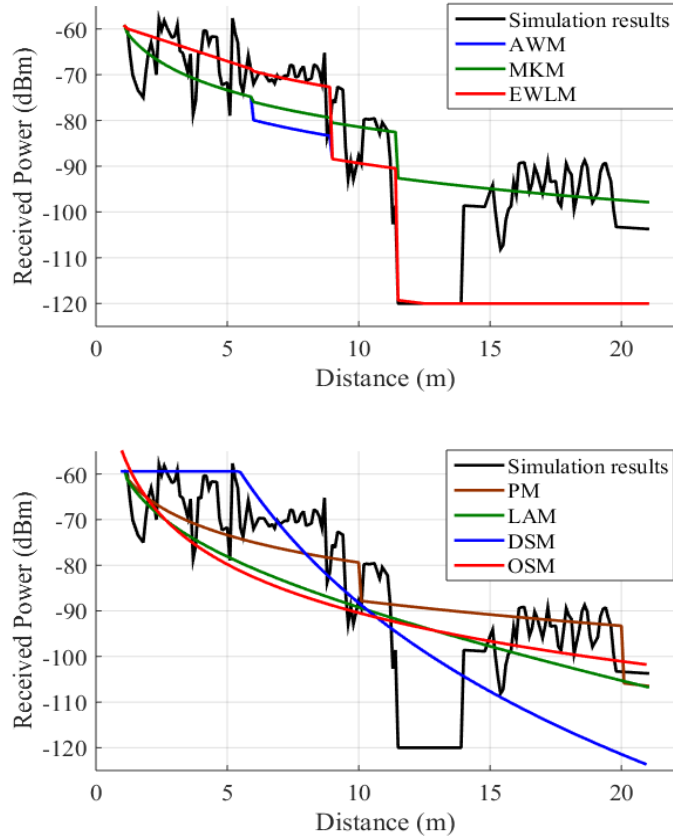
Figure 6: Indoor path loss prediction models comparisons at 60 GHz and circular polarization for a route in the environment.
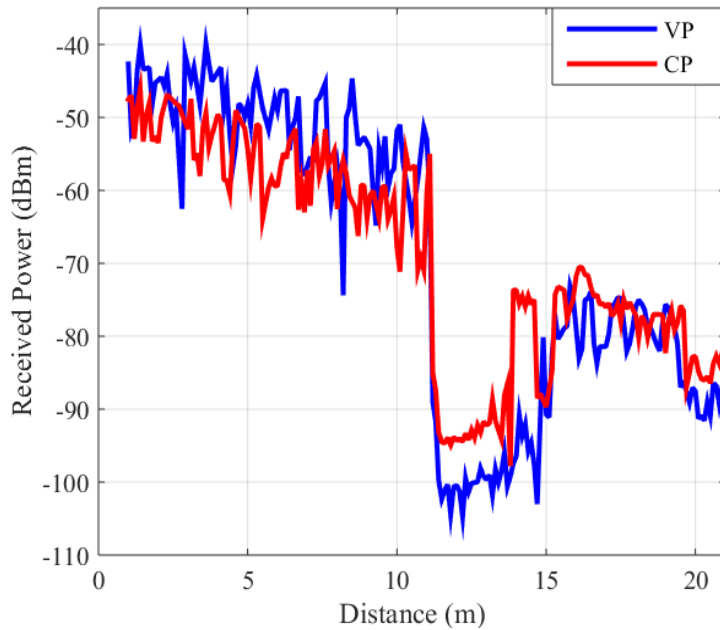
Figure 7: Received Power comparison between simulated VP and CP propagation at 28 GHz.
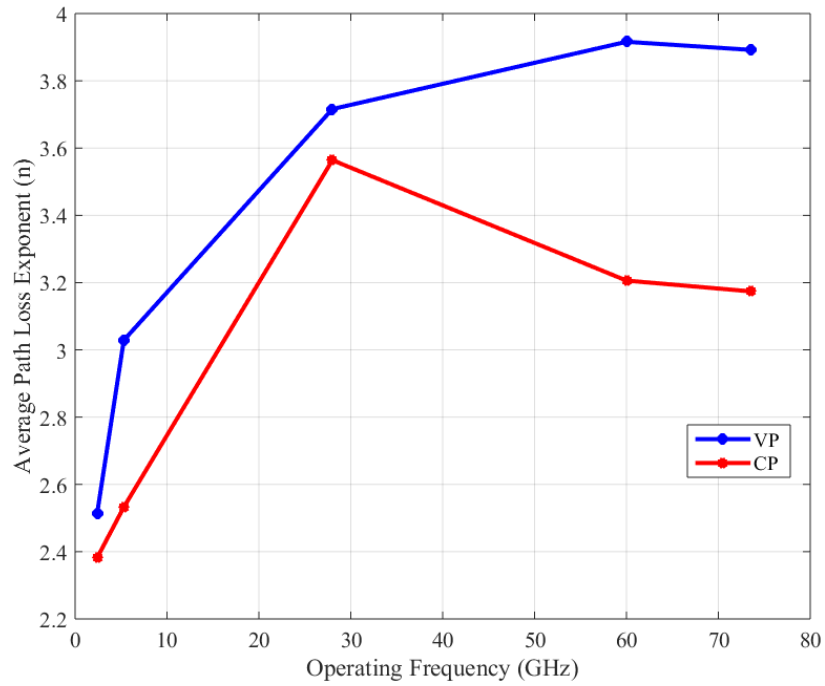
Figure 8: OSM path loss exponent relationship with operating frequency.
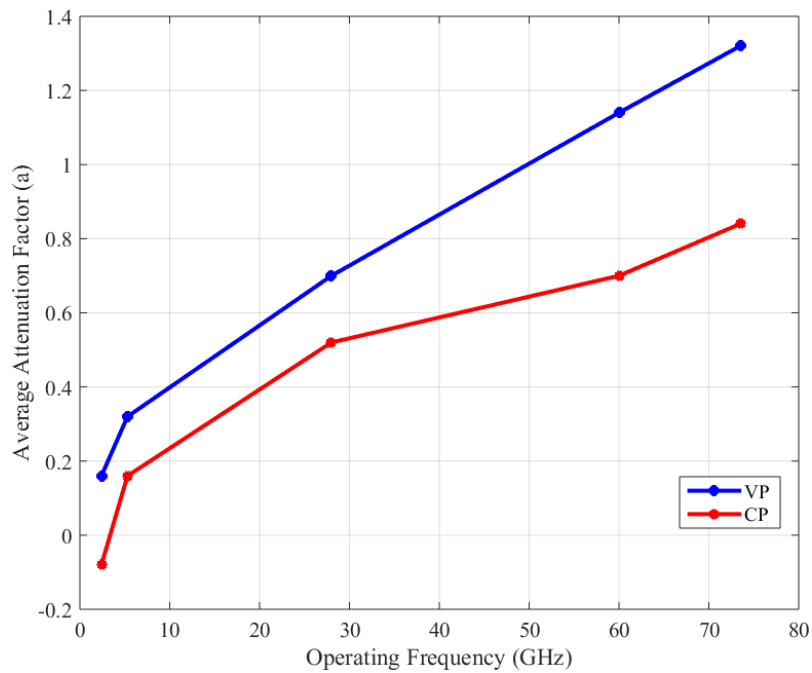
Figure 9: Linear attenuation factor relationship with operating frequency.
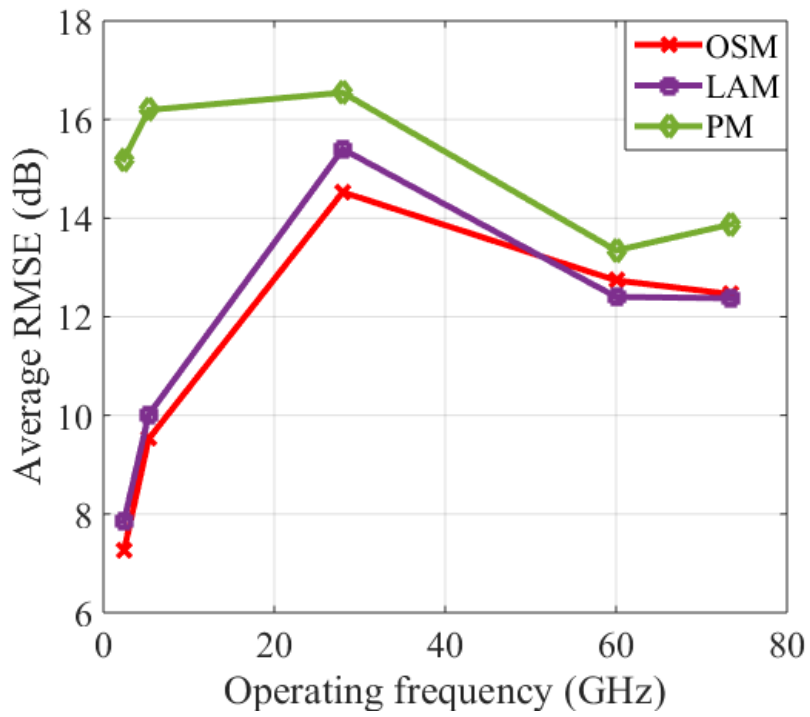
Figure 10: Performance comparison between LAM, OSM and PM.
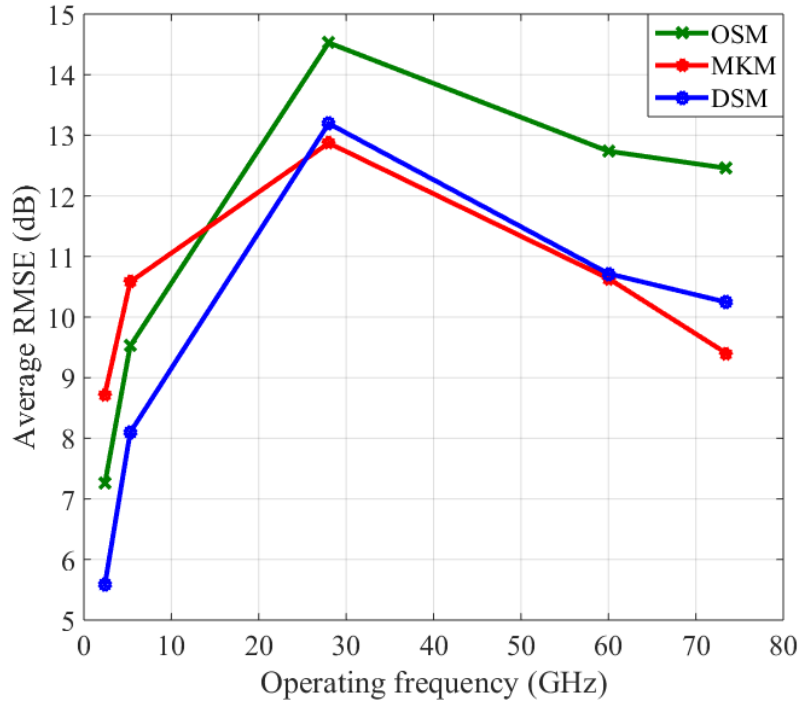
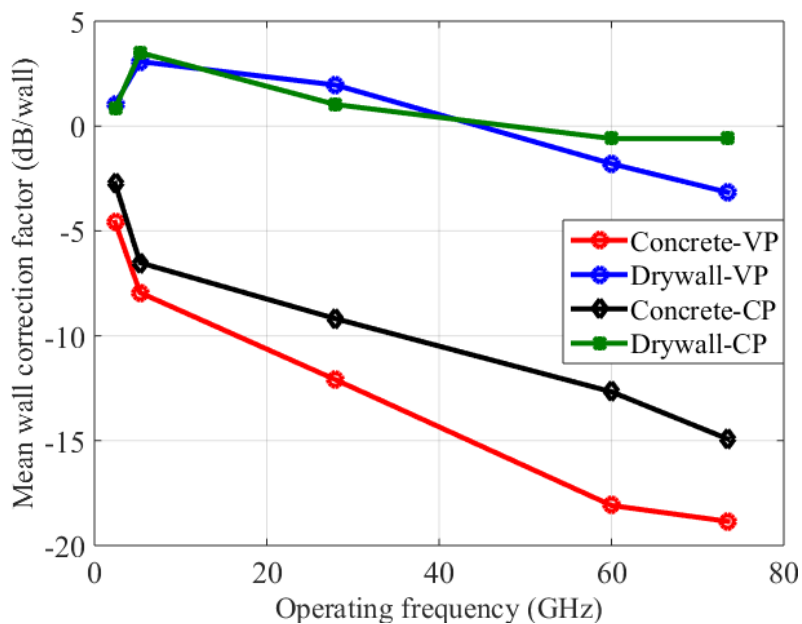**Figure 11**: Performance comparison between DSM, MKM and OSM.
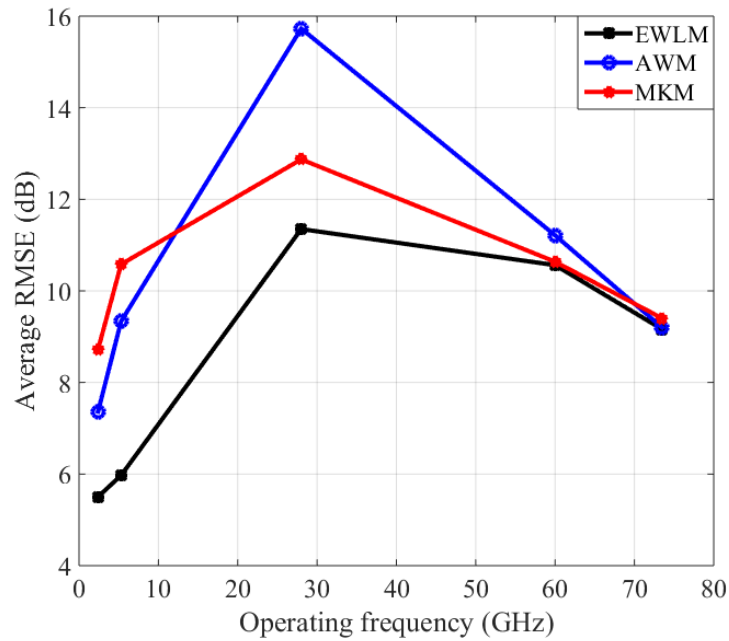
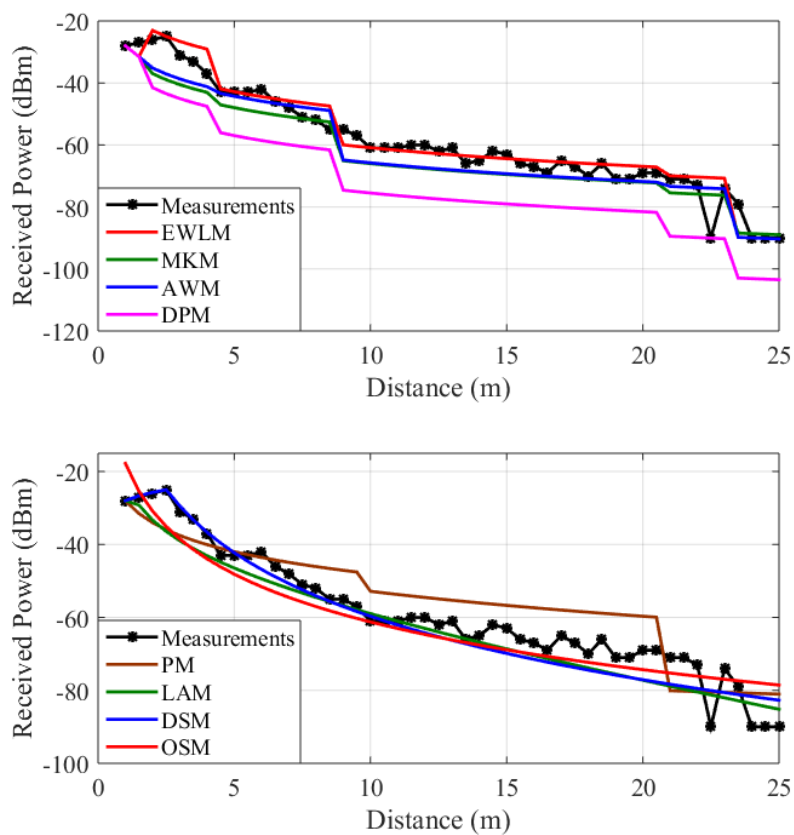**Figure 12:** Performance comparison between EWLM, AWM and MKM.
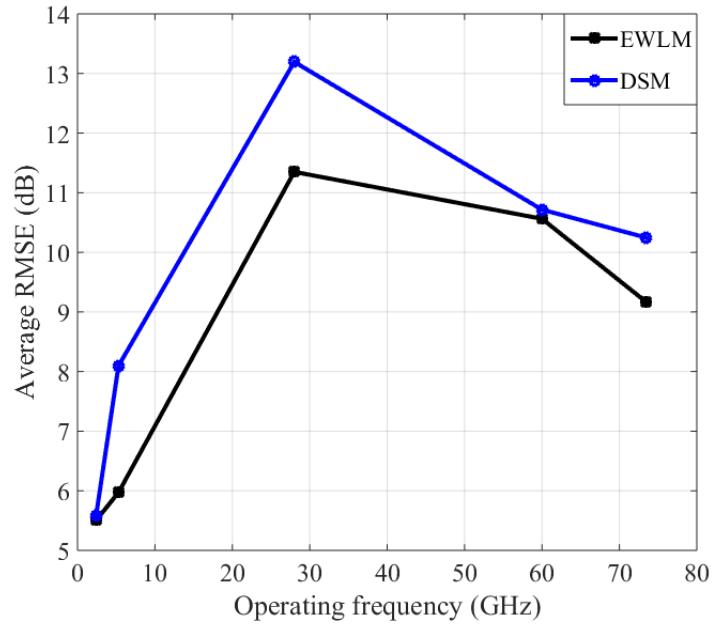
Figure 13: Performance comparison between EWLM and DSM.
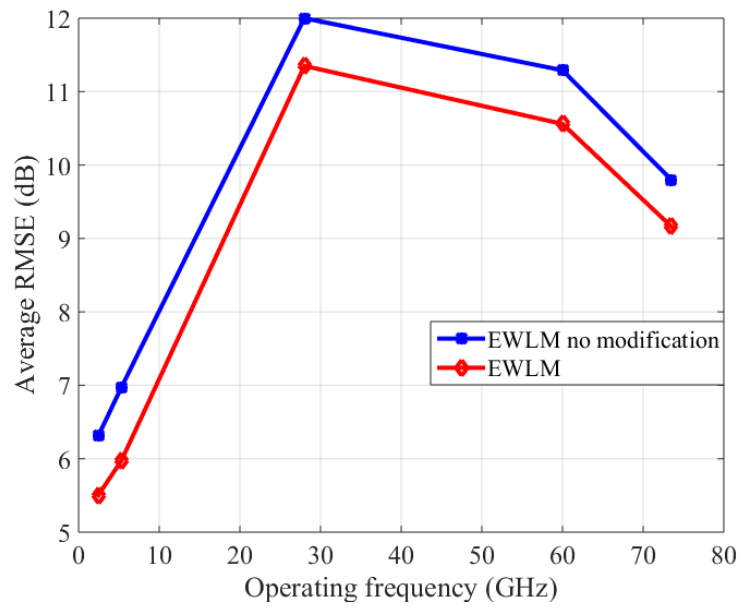
Figure 14: Enhancement on EWLM by considering effect of LOS propagation.

Figure 15: Mean wall correction factor relationship with operating frequency for concrete and drywall.

Figure 16: Indoor path loss prediction models comparisons at 5.3 GHz for route 2-2 in the environment.
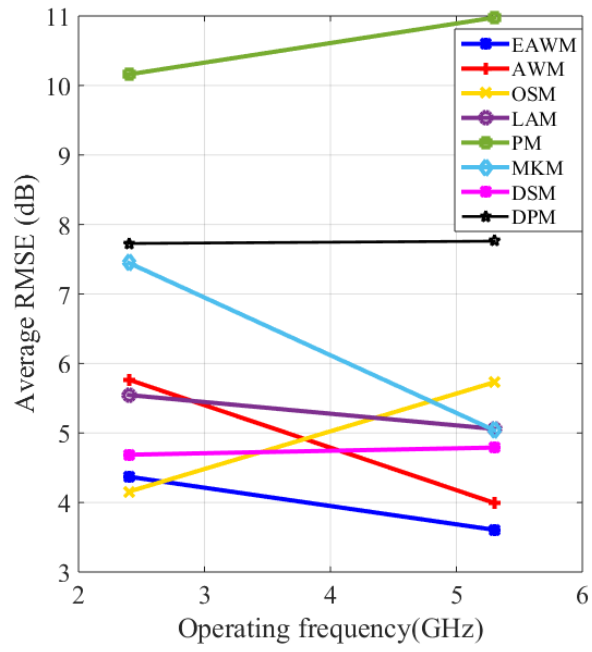
Figure 17: Average RMSE for all models.